Published online 24 November 2016

Nucleic Acids Research, 2017, Vol. 45, No. 2 ***1005–1014***
doi: 10.1093/nar/gkw1045

Engineering robust and tunable spatial structures with synthetic gene circuits

Wentao Kong[1,2], Andrew E. Blanchard[2,3], Chen Liao[1,2] and Ting Lu[1,2,3,*]

[1]Department of Bioengineering, University of Illinois at Urbana-Champaign, Urbana, IL 61801, USA, [2]Carl R. Woese Institute for Genomic Biology, University of Illinois at Urbana-Champaign, Urbana, IL 61801, USA and [3]Department of Physics, University of Illinois at Urbana-Champaign, Urbana, IL 61801, USA

Received August 04, 2016; Revised September 30, 2016; Editorial Decision October 19, 2016; Accepted October 20, 2016

ABSTRACT

Controllable spatial patterning is a major goal for the engineering of biological systems. Recently, synthetic gene circuits have become promising tools to achieve the goal; however, they need to possess both functional robustness and tunability in order to facilitate future applications. Here we show that, by harnessing the dual signaling and antibiotic features of nisin, simple synthetic circuits can direct *Lactococcus lactis* populations to form programmed spatial band-pass structures that do not require fine-tuning and are robust against environmental and cellular context perturbations. Although robust, the patterns are highly tunable, with their band widths specified by the external nisin gradient and cellular nisin immunity. Additionally, the circuits can direct cells to consistently generate designed patterns, even when the gradient is driven by structured nisin-producing bacteria and the patterning cells are composed of multiple species. A mathematical model successfully reproduces all of the observed patterns. Furthermore, the circuits allow us to establish predictable structures of synthetic communities and controllable arrays of cellular stripes and spots in space. This study offers new synthetic biology tools to program spatial structures. It also demonstrates that a deep mining of natural functionalities of living systems is a valuable route to build circuit robustness and tunability.

INTRODUCTION

Spatial pattern formation is one of the most remarkable capacities of natural living organisms (1). For instance, the social bacterium *Paenibacillus vortex* coordinates with each other to form spiral vortexes on agar plates (2); the embryo of *Drosophila melanogaster* develops into an adult fly under the guidance of spatially and temporally ordered morphogen gradients (3) and cheeta and zebra are coated with the patterns of spots and stripes on their skins accordingly (4). Owing to the ubiquity and versatility of pattern formation in nature, achieving an engineering ability of cellular pattern programming has been a major goal for the engineering of biological systems (5–11). Along this direction, there has been an array of recent synthetic biology efforts. Successful examples include programmed bull's eye patterns from synthetic producer–responder cells (12), synchronized oscillation and travelling waves among cells with coupled positive and negative feedback circuits (13), sequentially developed stripes of growing cells enabled by density-dependent chemotaxis (14), scale-invariance rings self-organized through the modulation of temporal dynamics of diffusible molecules (15), and others (16–19). Although these studies were primarily for proof-of-concept purposes, they offered highly valuable implications in multiple ways. First, following the 'build-to-understand' concept, the construction and characterization of patterning circuits yielded insights into the fundamental mechanisms of coordinated biological behaviors and spatial pattern formation of natural systems. Second, the resulting engineered gene circuits enriched the arsenals of synthetic biology for directing the spatial organization of cellular populations, which has the potential for applications in a variety of fields such as tissue engineering, biomaterial fabrication and biological computation.

To further foster their practical applications and deepen the understanding of fundamental design principles, synthetic gene circuits for pattern formation or any other purposes, need to possess two characteristic features, robustness and tunability. The former refers to a circuit's ability in maintaining its behaviors upon external and internal perturbations while the latter describes the extent to which a circuit can be tuned. With both features, a circuit will persistently execute its functionality under perturbations and, in the meanwhile, remain subjective to designed regulatory signals for behavioral modulation. To create such circuits, one promising strategy is to deeply mine the untapped functional capacities of natural living systems, as many natural organisms have evolved to acquire both features without costing a high degree of system complexity. In this paper,

*To whom correspondence should be addressed. Tel: +1 217 333 4627; Fax: +1 217 265 0246; Email: luting@illinois.edu

we present gene circuits for spatial band filtering that are developed by exploiting the natural dual signaling and antibacterial features of nisin, an antimicrobial peptide produced by *Lactococcus lactis* (20). The circuits are simple in design and construction but robust and tunable in functionality. Interestingly, with the robustness and tunability, the circuits not only generate persistent spatial ring structures but also confer the establishment of predictable spatial structures of synthetic communities and controllable arrays of cellular stripes and spots in space.

MATERIALS AND METHODS

Bacterial strains and growth conditions

Escherichia coli NEB-10β was used for cloning and plasmid construction. *Lactococcus lactis* K29 is a nisin producer used in the experiments. *Lactococcus lactis* NZ9000 is used as host for nisin responder strains in all cases. *Lactococcus lactis* strains are cultured in M17 medium with 0.5% glucose at 30°C. All plasmids were first constructed and sequenced in *E. coli* and then transformed into *L. lactis* by electroporation. Chloramphenicol was added at a final concentration of 10 μg/ml for *E. coli* and 5 μg/ml for *L. lactis* if necessary.

Cloning and plasmid construction

Gibson assembly was used to construct most of the plasmids. Oligos with overlapping regions for PCR amplification and Gibson assembly were listed in Supplementary Table S2. Nisin induced GFP expression plasmid (pleiss-PnisA-gfp) and RFP expression plasmid (pleiss-PnisA-rfp) were constructed by assembling a gfp fragment or mcherry fragment with the pLeiss:Nuc vector which contains the PnisA promoter (21). The plasmid for constitutively expressing GFP (pleiss-Pcon-gfp) was constructed by cloning gfpuv gene and the constitutive promoter of lcnA into pleiss-Nuc vector (22). The plasmid, pleiss-Pcon-rfp, was constructed by replacing gfp in pleiss-Pcon-gfp with mcherry. Constitutive promoters, P23, P32, P59 and P3a, were synthesized via gblock by IDT (Integrated DNA Technologies). Different versions of nisI expression plasmids were constructed by integrating constitutive promoters and nisI with the fragment of pSH71 replicon and chloramphenicol resistant gene from the pLeiss:Nuc plasmid. The nisin induced GFP expression plasmid with nisin immunity (pleiss-PnisA-gfp-P3a-nisI) was constructed by insertion of P3a-nisI downstream of gfp and separated by a T1T2 terminator. All the plasmids were constructed in *E. coli* and sequenced, and then transformed into *L. lactis* NZ9000 to test for their phenotypes.

Growth curve and GFP measurement

An inoculum of *L. lactis* NZ9000/pleiss-PnisA-gfp (iGS) was grown overnight to stationary phase and then transferred to fresh media at a 1:100 dilution. The new inocula were added with nisin to a final concentration of 3×10^{-5} to 30 IU/ml when their OD_{600} reached 0.3. After 5 h incubation, OD_{600} and relative green fluorescence were measured.

NisI expressing cells and GFP control cells were inoculated by a 1:100 dilution of the overnight cultures. When their OD_{600} reached 0.3, nisin was added to the cultures at a final concentration of 0.01–3000 IU/ml. The cultures were incubated at 30°C for another 5 h and then cell numbers were counted by dilution and plate pouring.

Nisin induced patterns by agar diffusion through wells and filter papers

A double layer agar diffusion method was used to demonstrate nisin induced pattern. First, a bottom layer was prepared by mixing 100 μl of nisin responder cells (iGS or iGR) with 25 ml of molten GM17 agar (1% soft agar) and pouring to a 150 mm plate. Half an hour later, the bottom agar was overlaid with an additional 25 ml of 50°C molten soft agar. Meanwhile, a 96-well PCR plate (well maker) was placed in the upper layer to make wells. Another half hour later, the PCR plate was removed, and 15 μl of standard nisin solution (10–100 IU/ml) were added into wells. After incubation at 30°C for 10 h, images were taken of the plates.

Agar plates were made by mixing 100 μl of overnight cultures of *L. lactis* NZ9000/ pleiss-PnisA-gfp (iGS) and 30 ml of molten GM17 agar and pouring to a 150 mm plate. Filter papers (Whatman) were cut to form different patterns. Then these cut papers (masks) were immerged into 10 IU/ml of nisin solution and put on the surface of the plates. Plates were incubated at 30°C for 20 h and then images were taken.

Robustness test for nisin induced programmed patterns

A standard experimental setting for nisin induced programmed pattern is 1× GM17, 1% agar, natural pH of GM17 (6.86), 30°C and aerobic. To examine the robustness of programmed spatial ring formation in response to environmental factors, the M17 concentration (0.1×–4×), agar concentration (0.75–2.25%), pH (4.5–8.8), temperature (22–40°C) and oxygen (aerobic or anaerobic) were chosen as environmental variables for pattern formation. Briefly, fifty microliters of overnight cultures of iGS were mixed with 20 ml of molten GM17 agar (M17 concentration, agar concentration or pH was adjusted accordingly). Then, the mixture was poured into a 9 mm plate, and a PCR plate was placed on it to make wells. After solidification, 15 μl of 25 IU/ml of nisin were added to the well and the plates were incubated in aerobic or anaerobic incubators at different temperatures. Images were taken after 10 h of incubation. To examine the system's robustness to host alterations, the plasmid pleiss-PnisA-gfp was transformed into *Lactobacillus casei* BL23 (nisRK integrated in its chromosome). The resulting strain, *Lb. casei* BL23/pleiss-PnisA-gfp, was used as responder cells for the formation of nisin induced patterns under the standard experimental condition setting except incubation at 37°C. To examine the effect of plasmid replication origin on pattern formation, the PnisA-gfp cassette was amplified from pleiss-PnisA-gfp and cloned into medium to the high copy number plasmid pCCAMβ1 (pAMβ1 origin) (23) and the low copy number plasmid pMG36e (pWV01 origin) (24). The primers for cloning procedure were listed in Supplementary Table S2. *Lactococcus lactis* NZ9000 was transformed with the new plasmids and subsequently used to perform pattern formation experiments according to the standard settings.

Nisin induced patterns at the single cell level

A thin-layer GM17/Cm agar plate was made by pouring 8 ml of molten GM17 agar plus 5 μg/ml of chloramphenicol into a 90 mm plate. The plate was first allowed to cool down at room temperature for half an hour. Then a 1 × 1 cm agar pad was cut from the plate and 0.2 μl of 100 IU/ml nisin was added on the center of the agar pad. After the nisin diffused into the agar pad, 5 μl of nisin responder cells were dropped onto the agar pad. The agar pad was then inverted and put in a 35 mm glass bottom dish. After 12 h of incubation at 30°C, images were taken by a fluorescent microscope.

Nisin producer directed pattern formation

Nisin responder cells were grown to early stationary phase and then diluted with GM17 medium to an OD_{600} of 0.2. Twenty milliliters of molten GM17 agar (1% agar) were poured into a 90 mm plate. After solidification for 30 min, 75 μl of diluted nisin responder cells were added onto the plate. After the droplet dried 0.25 μl of early stationary phase of nisin producer culture was added onto the center of the dried nisin responder cells. Then the plates were incubated at 30°C for 12–14 h and images were taken using an Axio Zoom V16 Microscope.

To test the robustness and tunability of our circuit in the new setting, nisin responder cells with different densities (OD_{600} = 0.05, 0.1, 0.2, 0.5 and 1) were used to perform the producer directed patterning experiment. A control strain NZ9000/pleiss-nuc was mixed with nisin responder cells (total OD_{600} = 0.2) at ratios from 0% to 100% to test the disturbance of the responder by a nonresponding strain. Additionally, two species of nisin responders (OD_{600} = 0.2) were mixed at ratios of 5:1 to 1:5.

Mixed population pattern formation

Nisin producer and responder cells were first grown to an early stationary phase. Cells were mixed at a ratio of 20:1, 1:1, 1:20, 1:100, 1:500 and 1:50 000 (producer: responder) and diluted to an OD_{600} of 0.2. Then 75 μl of diluted cell mix of nisin producer and responder was added onto the GM17 agar plate (1% agar). The droplets were allowed to dry and then they were incubated at 30°C for 12 h. Images were taken using an Axio Zoom V16 Microscope.

Program controllable stripe and spot patterns driven by nisin producers

To generate stripe patterns, PiG and iRS/cRS were used as nisin producer and responder cells. Forty microliters of overnight cultures ($OD_{600} \approx 3$) of the producer (PiG) or responder (iRS or cRS) cells were spread on 90 mm of GM17/Cm agar plates. The PiG plates were incubated at 30°C for 24 h before use to allow the surface of the agar to have more cells than iRS or cRS plates. A razor blade was dipped in bacteria by gently touching the surface of the plate seeded with nisin responder. The blade was then used to stamp stripes with 3 mm spaces in parallel on a new GM17/Cm plate (2% agar). Subsequently, a blade dipped in PiG cells was used to stamp stripes in a direction perpendicular to the nisin responder with different distances (4, 13, 20 and 40 mm). The plates were incubated at 30°C for 16 h and fluorescent images were taken. To generate kaleidoscope like spot patterns, cultures of the nisin producer (PiG) were diluted or concentrated to different cell densities (OD_{600} = 0.0001, 0.2, 1, 6 and 10). Then 3 μl of nisin responder (iRS or cRS, OD_{600} = 0.2) was dripped onto vertices of hexagon shapes with an 8 mm length of the side in a honeycomb structure on GM17/Cm agar plate (1% agar). Different volumes (0.5 μl of culture with OD_{600} = 0.0001, 1 μl of culture with OD_{600} = 0.2, 3 μl of culture with OD_{600} = 1, 7.5 μl of culture with OD_{600} = 6 and 9 μl of culture with OD_{600} = 10) of PiG cells were added onto the center of hexagon. The plates were incubated at 30°C for 16 h to form the patterns.

Mathematical modeling

Differential equations were used for model development. Custom-tailored C++ code was developed in order to implement computational simulations. Parameters were chosen based on previous literature and our own experimental data. See Supplementary Mathematical Modeling for a detailed description about the model construction, parameters and computational methods.

RESULTS

Creating band-pass patterns in space by exploiting nisin's dual functionality

Our circuit (Figure 1A) consists of a constitutively expressed two-component system *nisRK*, responsible for nisin signal transduction, and a green fluorescence protein (*gfp*) reporter controlled by the nisin-inducible promoter P_{nisA}. This simple design is based on the dual signaling and antibacterial features of the bacteriocin nisin (25) (Figure 1B): For a cell carrying the circuit, it shall have no fluorescence response when the nisin concentration is too low (left panel); it can glow when in the presence of an appropriate nisin level that triggers signaling (middle panel); however, when the nisin concentration is too high, the cell will be killed by nisin because of its antibiotic feature, resulting in a failure in fluorescence expression (right panel). Therefore, for an exponentially distributed profile of the nisin gradient (Figure 1C, top panel), the engineered cells plated along the X axis shall have a sigmoidal rate of survival (Figure 1C, second panel) because of the antibiotic feature of nisin. At the same time, the fluorescence intensity of the cells shall follow an inverse sigmoidal distribution, owing to the need for nisin in gene expression induction (Figure 1C, third panel). With both the antibiotic and signaling features, the two opposing effects shall be superposed for every cell, leading to a band-pass pattern in space (Figure 1C, bottom panel). Notably, in contrast to systems that generate emergent patterns (e.g. Turing patterns), our circuit creates programmed spatial patterns responding to external nisin gradients.

To create such a patterning system, we first validated the dual functionality of nisin, by culturing the engineered strain iGS (*L. lactis* NZ9000 strain loaded with a nisin inducible GFP reporter) in liquid medium (GM17) supplemented with nisin, measuring the culture growth (optical density (OD)) and total green fluorescence intensity, and

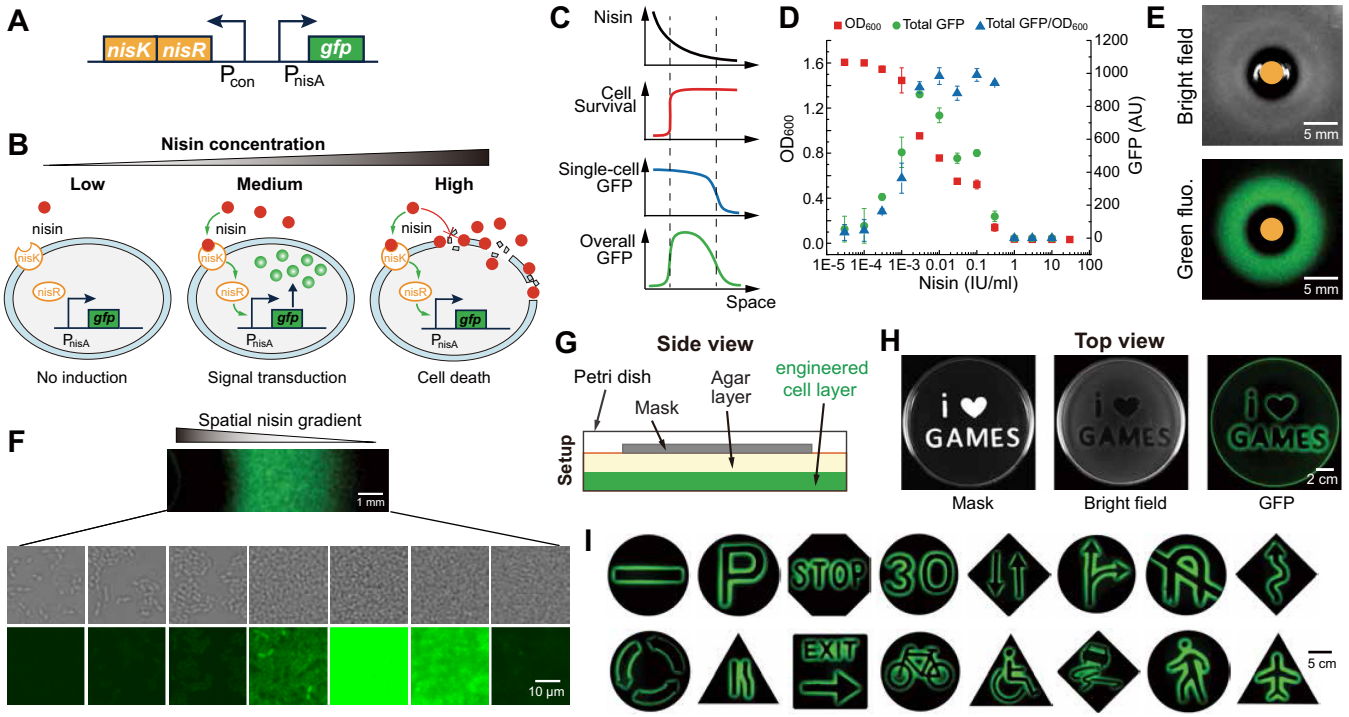

Figure 1. A simple gene circuit that produces robust spatial band-pass patterns. (**A**) Circuit design. The circuit consists of a two-component nisin signaling system (*nisRK*) and a nisin inducible green fluorescence reporter (*gfp*) only. (**B**) Differential responses of the circuit to external nisin. A low level of nisin concentration fails to trigger fluorescence production or cell death, resulting in cells viable but non-glowing. A medium level of nisin concentration induces the expression of green fluorescence gene without killing the cells, enabling the cells to glow. A high level of nisin causes cell death, resulting in a failure in producing fluorescence. (**C**) Schematic of the band-pass behavior in space. (**D**) Confirmation of the signaling and antibacterial features of nisin in liquid settings ($n \geq 3$). (**E**) Spatial band-pass pattern emerged from a cellular lawn loaded with the circuit. A green fluorescence stripe forms around a nisin-emitting well (orange well). Between the stripe and the well is the inhibition zone caused by the antibacterial feature of nisin. Scale bar: 5 mm. (**F**) Single-cell images of the band-pass populations across space. Top row: brightfield images; bottom row: fluorescence images. Scale bar: 10 μm. (**G**) Experimental setup for remote pattern printing on a solid agar plate. The cellular lawn growing at the bottom of the plate is covered by a solid agar layer; a mask soaked with nisin is placed on top of the agar. (**H**) Demonstration of pattern printing. The pattern of the mask (i love (heart) GAMES) was remotely printed to the cellular lawn at the bottom through nisin diffusion, producing a glowing structure that reflect the edge of the mask pattern. Scale bar: 2 cm. (**I**) Various traffic sign patterns created using the procedure described in panel G. Scale bar: 5 cm.

calculating the normalized fluorescence intensity (i.e. total fluorescence divided by OD) (see Materials and Methods for details). Our results (Figure 1D) showed that the cellular growth rate, reflected by OD, decreases with the level of nisin in the culture (red squares); meanwhile, the normalized fluorescence level which corresponds to nisin signaling, increases with nisin (blue triangles). Notably, the normalized fluorescence level collapses to zero when the nisin concentration is at a level of 1.0 international unit (IU)/ml or higher, attributed to the fact that cellular growth is prohibited by nisin at that level. The total fluorescence intensity (green circles) changes from low to high and to low again with respect to nisin, suggesting that the circuit confers a band-pass behavior in liquid.

We then examined the green fluorescence pattern of cells in space where nisin distribution is heterogeneous. We plated a lawn of engineered cells on a solid agar plate which contains a well in the center filled with nisin (nisin dissolved in pH 2.0 HCl/1% Tween 20) and incubated the plate at 30°C (see Materials and Methods for details). After 10 h, we found that a clear inhibition zone formed around the well (Figure 1E, top panel, brightfield image) and a symmetrical ring-like structure formed in space (Figure 1E, bottom panel, fluorescence image). The side view of the structure and the time course of ring formation are shown in Supplementary Figures S1 and S2 accordingly. Notably, although no fluorescence was observed in both the areas close and distant from the well, the underlying causes are different: the former resulted from the absence of living cells due to growth inhibition by a high dose of nisin; by contrast, the latter was caused by the lack of GFP expression because of the insufficiency of nisin concentration for signaling. These results demonstrated that our circuit successfully directed the emergence of spatial band-pass patterns of the populations. In addition, we confirmed the necessity of nisRK for signal transduction and ring structure formation (Supplementary Figure S3). To further confirm the band-pass structure, we examined both cellular growth and overall fluorescence of the cellular lawn at the single-cell level. Figure 1F shows the bright field and fluorescence images of the cells across the nisin gradient. Consistent with our design, the cellular survival indeed increased with the distance from the nisin source while the overall fluorescence intensity follows a low-high-low pattern.

Next, we tested the feasibility of creating complicated spatial structures with the engineered circuit. As shown in Figure 1G, we set up our patterning environment where a cellular lawn was planted at the bottom of a plate, an agar

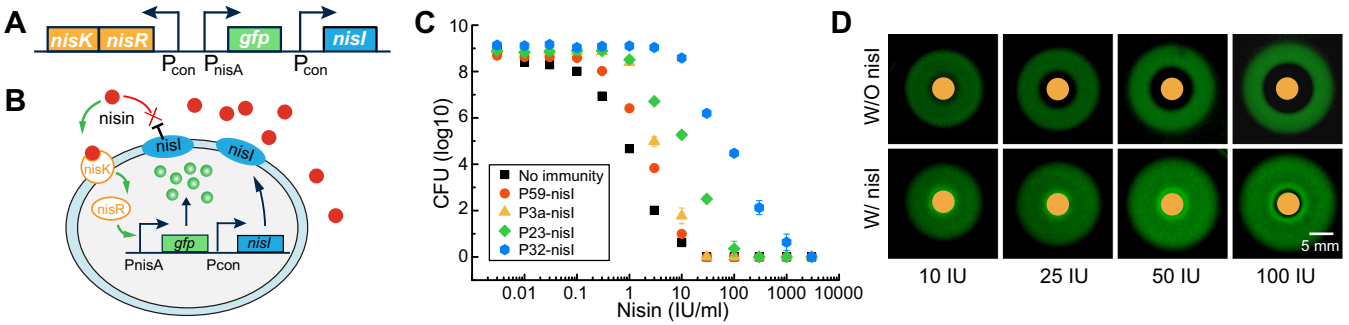

Figure 2. Pattern fine-tuning with cellular nisin immunity and external nisin concentration. (**A**) Circuit design. A nisin immunity gene (*nisI*) is introduced into the original circuit in Figure 1A to alter cellular sensitivity to nisin. (**B**) Schematic illustration of enhanced nisin immunity conferred by the expression of the nisin immunity gene. (**C**) Colony forming unit counting as a function of external nisin for cells containing different levels of nisin immunity. Data are presented as mean ± SD ($n \geq 3$). (**D**) Spatial band-pass patterns emerged from populations with or without nisin immunity. For the cellular lawns containing the nisin immunity gene (bottom row), the inner diameters, defined by cellular resistance to nisin, are much smaller than those of the cells lacking nisin immunity (top row). Here, the orange circles are wells loaded with nisin. Scale bar: 5 mm.

layer in the middle, a paper mask, soaked with nisin, on the top (see Materials and Methods for details). We found that, for a plate covered with a mask that has a pattern of 'i love (heart) GAMES' (Figure 1H, left panel), the pattern was able to be remotely printed to the cellular layer at the bottom (Figure 1H, middle panel) after 20 hours of incubation (bright field image). In addition, we found that, conferred by the band-pass feature of the circuit, the cellular lawn showed a clean fluorescence pattern that mimics the edge of the mask (Figure 1H, right panel), showing that the circuit remains functional for complicated patterns. To further demonstrate its utility, we made a set of masks representing different traffic signals, resulting in a total of 16 distinct traffic patterns as shown in Figure 1I.

Synthetic circuits are robust against environmental and cellular context variations

A demanding characteristic of synthetic circuits is functional robustness, a property that allows the circuits to maintain their behaviors despite external and internal perturbations (26). For our circuit, successful creation of the 16 patterns (Figure 1I) has indicated that it is functionally robust. To systematically evaluate its robustness, we performed a series of spatial patterning experiments under altered environmental conditions. We varied the formulation of the medium composition by changing its nutrient concentration from 0.1× to 4× (Supplementary Figure S4A) and agar concentration from 0.75% to 2.25% (Supplementary Figure S4B). We also changed the pH of the agar plates from 4.5 to 8.8 (Supplementary Figure S5A), the incubation temperature from 22°C to 40°C (Supplementary Figure S5B), and the oxygen availability from diminished to abundant (Supplementary Figure S5C). Through a total of 39 perturbations, we found that, although the details of the resulting patterns (e.g. their diameters and fluorescence intensities) may vary, the circuit was able to persistently generate the ring-like structures. Thus, these experiments demonstrated that our circuit is robust against environmental perturbations. In addition, we examined how the circuit responds to the variations of cellular contexts, such as the host organism and plasmid copy number. By changing the host from a *L. lactis* strain (NZ9000) to a *Lactobacillus casei* strain (BL23), we found that the circuit in different hosts responded similarly to external nisin concentrations (Supplementary Figure S6A and the top row of Figure 2D), demonstrating that it is robust against host organism variations. We also altered the circuit's copy number by replacing the origin of replication pSH71 with pAMβ1 and pWV01 (Supplementary Figure S6B), confirming that the circuit remains persistent upon copy number perturbations. Furthermore, we mixed the engineered strain iGS with the control strain (NZ9000/pleiss-Nuc) during pattern formation (Supplementary Figure S7) and, again, found that the ring structures continued to emerge. Together, the above experiments demonstrated that our synthetic circuit is functionally robust against both environmental and cellular context perturbations.

Tuning the patterns by varying cellular immunity and external nisin gradient

Our circuit is robust in generating ring-like patterns; however, does the robustness of the circuit compromise its tunability? Here, we sought to engineer a high degree of tunability into the circuit by, again, utilizing the natural functionality associated with nisin. Specifically, we introduced *nisI* (20), a gene that confers nisin immunity, to the engineered strain to fine-tune the patterns (Figure 2D). Our design is based on the fact that the inner diameter of the band-pass patterns is characterized by the strain's sensitivity to nisin (Figure 1C, second panel) and, thus, altering the strain's immunity to nisin can change the inner diameter of the band. We therefore constructed four circuit variants (P59-nisI, P3a-nisI, P23-nisI, P32-nisI) that possess different expression levels of the immunity gene (Supplementary Table S1). Our colony forming units (CFU) assays (Figure 2C) showed that the circuit variants all have an increase in nisin resistance, with their specific levels determined by the strength of the promoters controlling *nisI*.

To confirm the circuit's tunability, we conducted a set of patterning experiments using the nisI-expressing variant (Figure 2A) and the original circuit (Figure 1A). Our results showed that, for the cellular lawn harboring the original cir-

Table 1. Nisin producer and responder strains used in spatial patterning experiments

Strain	Functional characteristics
PiG	Nisin producer; self-inducible GFP expression; resistant to nisin
iGS	Nisin responder; nisin-inducible GFP expression; sensitive to nisin
iRS	Nisin responder; nisin-inducible RFP expression; sensitive to nisin
iGR	Nisin responder; nisin-inducible GFP expression; resistant to nisin
cGS	Nisin responder; constitutive GFP expression; sensitive to nisin
cRS	Nisin responder; constitutive RFP expression; sensitive to nisin

cuit (Figure 2D, top row), the inner and outer diameters of the bands increase with the level of nisin in the well (orange circles) (Quantitative data are shown in Supplementary Figure S8). The reason is that, for the given nisin sensitivity and signaling threshold defined by the circuit, increasing the nisin concentration at the source pushes both the survival and signaling profiles away from the source (Figure 1C). By contrast, for the cells with increased nisin immunity (P3a-nisI), the outer diameter increases with nisin concentration while the inner diameter remains almost the same (Figure 2D, bottom row), demonstrating that altering cellular immunity to nisin confers tunability to the patterns. It is noteworthy that the inner diameter of the resistance-enhanced cells will increase eventually when the nisin level is higher than cellular immunity. Thus, our patterns can be controlled by combinatorial modulation of cellular nisin immunity and environment nisin level.

Directing fine controllable patterns with nisin-producing bacteria

In natural living systems, morphogen gradients governing pattern formation are often established by cells rather than external control. We thus further tested circuit robustness by examining spatial population patterns driven by nisin-producing bacteria (producers). Figure 3A shows spatial structures formed by five different sets of nisin responsive cells (responders, listed in Table 1). Notably, the responders were driven by the same producer PiG, a wild-type nisin producing strain (K29) loaded with a GFP reporter, and each sector here corresponds to a specific experiment. We found that the lawns of the responders iGS and iRS, the NZ9000 strain loaded with the original circuit (Figure 1A) and inducible reporters, produced band-pass patterns (Sectors 1 and 2) similar to those directed by external nisin (Figure 1E). By contrast, for the responder with an enhanced immunity (iGR), the inner diameter of the patterns has almost disappeared (Sector 3). For comparison, those sensitive to nisin but capable of constitutive fluorescence production (cGS and cRS) generated homogeneous structures except for the gap areas close to the producers (Sectors 4 and 5). Here, the gaps are caused by the antibiotic activity of nisin; the homogeneous patterns are due to constitutive fluorescence expression. A nisin producer deficient in GFP production was also tested for the same set of experiments and similar results were obtained (Supplementary Figure S9).

Complex patterns often involve multiple types of populations. Thus, we evaluated the utility of our circuit in directing the pattern formation of multiple responder species (Figure 3B) (Separate green and red channels are shown in Supplementary Figure S10). Our results showed that a mixed lawn of the two nisin-inducible fluorescence responders, iGS and iRS, yielded a mixed green and red circular band along the radius (Sector 1). When the fluorescence reporter of one of the responders was changed from inducible to constitutive (iGS replaced by cGS or iRS by cRS), the corresponding well-mixed band structure was shifted to a three-section profile including no fluorescence close to the producers, mixed fluorescence in the middle, and single uniform fluorescence (green or red) at a large radius (Sectors 2 and 3). In addition, when both responders expressed fluorescence constitutively (cGS and cRS), a homogeneous pattern emerged in the space outside of the non-fluorescent area close to the producer cells caused by nisin inhibition (Sector 4). Here, nisin immunity continued to confer a tunability for pattern characteristics. Sector 5 shows that, when one of the responders was given an increased nisin immunity (iGS replaced by iGR), green fluorescence emerged in the area close to the producer. Compared to the mixed-color band in Sector 1, the appearance of the green zone was attributed to the enhanced immunity of the green responder (iGR). Lastly, by replacing the nisin inducible, red responder strain (iRS) with a constitutive version (cRS), the area away from the source turned from void to red (Sector 6). For this set of experiments, we noticed that there were minor differences for the non-fluorescence gaps between producer and responder cells for different settings, which can be explained by the growth difference of the corresponding responders (Supplementary Discussion and Figure S11). We also examined the patterns of various responder cells when there is no nisin producer (Figure 3C), ruling out the possibility that the observed patterns were caused by the variations of gene expression among the cells. Collectively, these experiments confirmed that our synthetic circuits are persistent in generating complex band-pass patterns for multiple responders. Additionally, we evaluated the circuits by varying the initial cell density (Supplementary Figure S12), mixing ratio and relative abundance (Supplementary Figures S13 and S14) of the responders for different producer-responder settings. The results showed that the circuits remain robust and controllable.

To quantitatively characterize the programmed patterns, we developed a mathematical model that mimics the spatial developmental processes of the engineered populations (see Supplementary Mathematical Modeling for the details of our model). The model utilizes reaction-diffusion equations to describe bacterial population dynamics and nisin diffusion, as well as the interactions between nisin, gene expression and cell growth. By fitting the model parameters to the experimental data obtained above, the model was able to successfully reproduce the patterns generated in our experiments. Figure 3D and E show the patterns of single- and two-species responders and Figure 3F shows the pattern from the control cases, agreeing well with the experimental data in Figure 3A–C accordingly (see Supplementary Figures S15–S17 for comparison). In addition, we reproduced the time course of the pattern formation in Supplementary Figures S18 and S19.

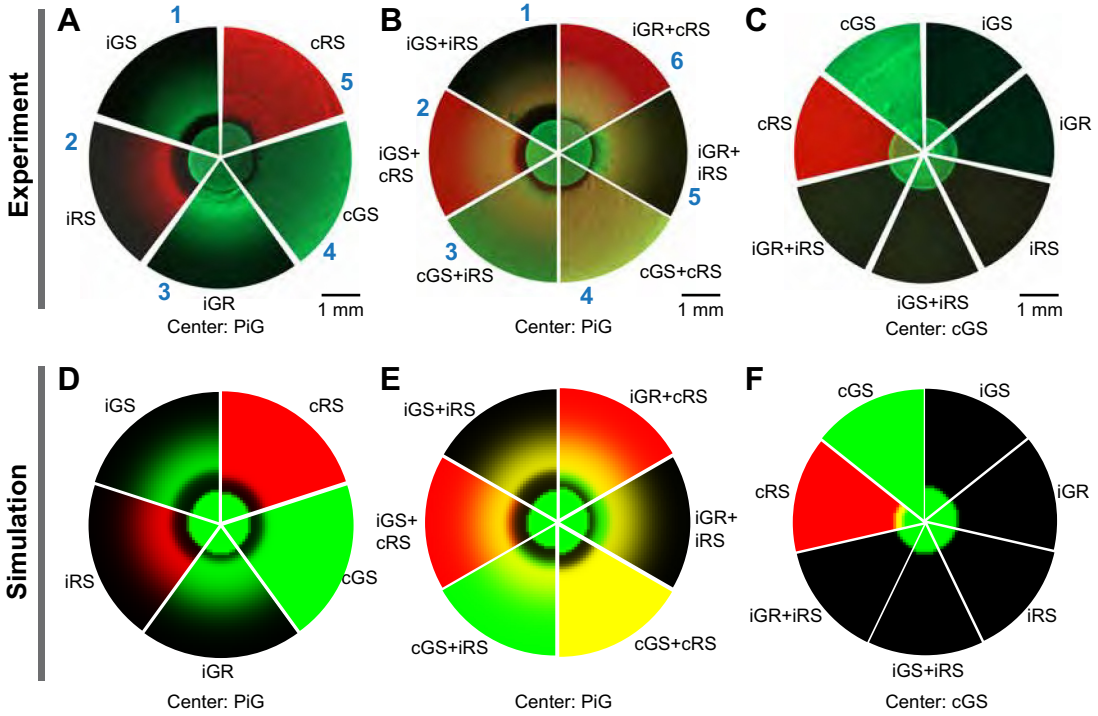

Figure 3. Various spatial patterns directed by nisin-producing bacteria. (**A–C**) Experimentally observed patterns of cellular populations directed by nisin producing bacteria. (**A**) Patterns of single-species responder populations. (**B**) Patterns of mixed, two-species responder populations. (**C**) Controls. Each experiment was repeated at least three times. Representative images from experiments are shown. The details of the responder and producer cells are available in Table 1. (**D–F**) Patterns emerged from the simulations of a mathematical model. The settings are identical to those of the experiments (A–C).

Harnessing the circuits to establish predictable spatial structures of synthetic communities

One ultimate goal of synthetic biology is to generate predictable dynamics and function with engineered gene circuits. Here, we sought to test whether our circuits can be used to generate predictable structures of synthetic bacterial communities, one emerging direction of synthetic biology that has lately attracted significant interest and shown compelling potential (27–29). Using the above model without changing its parameters and initial conditions of randomly distributed cell populations (Supplementary Mathematical Modeling), we explored the developmental processes of well-mixed bacterial communities plated on agar. Figure 4A and Supplementary Figure S20 show the emerged patterns of two-species consortia from simulations, suggesting that initial species composition (Row 1: PiG and iRS; Row 2: PiG and cRS; Row 3: cGS and cRS, and Row 4: cGS and iRS) and relative abundance (Columns 1–6: 20:1, 1:1, 1:20, 1:100; 1:500; 1:50 000) are both defining factors that specify the pattern characteristics (see Supplementary Figure S21 for the initial cell densities).

To test these predictions, we performed a series of pattern formation experiments by using the same procedure as in the simulations. Row 1 of Figure 4B shows the emerged patterns of a cellular lawn that consisted of a green nisin producer (PiG) and a nisin-sensitive responder capable of nisin-inducible RFP expression (iRS). Here, the producer and the responder were well mixed when initially plated on the agar. Over time, the resulting cellular lawn developed into a homogeneous green pattern when the producer-responder ratio was equal to one or larger (1:1 and 20:1), owing to the growth inhibition of the responder by the nisin secreted by the producer as well as the higher initial abundance of the producer. When the ratio was dropped to 1:20, void clusters (no fluorescence areas) emerged in the space, which was due to the fact that the nisin producer (green) was able to outcompete the responder (red) during pattern development but unable to fully occupy the space initially occupied by the responder. As the producer-responder ratio decreases, green–red coexistence started to emerge when the ratio fell into a fine-balanced regime (1:100 and 1:500). In this case, the producer abundance was low enough to allow the responder cells to grow and yet high enough to yield sufficient nisin for triggering the red fluorescence production of the surrounding responder cells. A pattern of sparse green spots (no red fluorescence) developed when the producer-responder ratio drops to an extremely low level (1:50 000), due to the fact that in this scenario, although the producer cells continue to produce nisin, the level of nisin they emitted was not enough to light up the entire population of the responders across space.

In addition, we studied the spatial self-organization of the consortium composed of the producer PiG and a nisin sensitive responder that constitutively expresses RFP (cRS). As shown in Row 2 of Figure 4B, the resulting patterns are different from those of the PiG-iRS community (Row 1) in two ways: first, the producer-responder balance that enables green-red coexistence is shifted to the left, i.e. a higher ratio value; second, the responder cells remain red even at the extremely low producer-responder regime (1:50 000). Here,

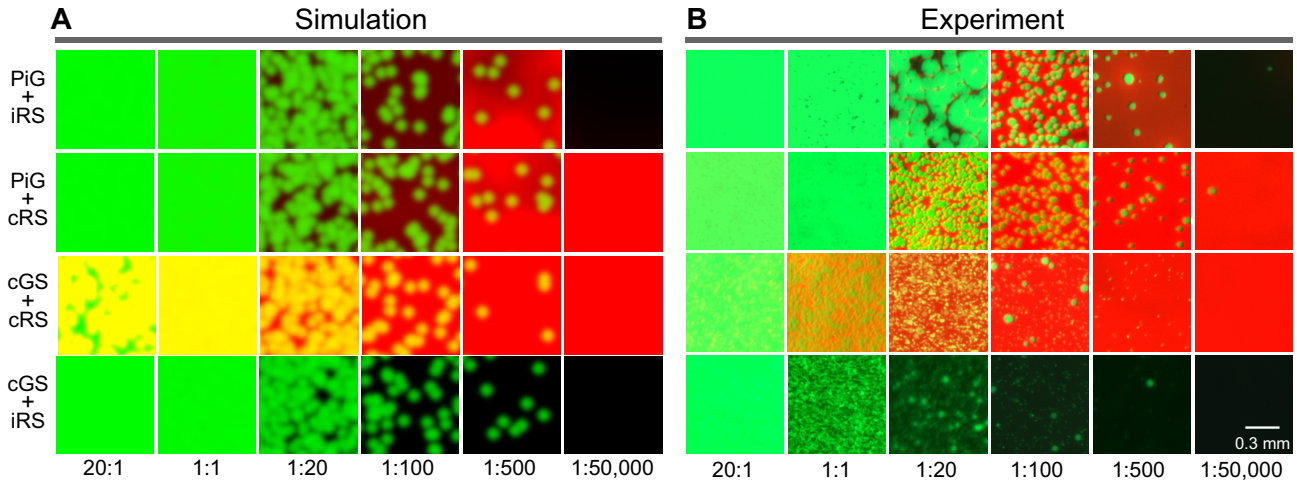

Figure 4. Autonomous emergence of distinct but predictable spatial structures from mixed bacterial populations. (**A**) Spatial patterns of bacterial consortia from the predictions of our computational model. Qualitatively distinct patterns develop as the species composition and initial relative abundance are varied. (**B**) Experimental validation of spatial structures of bacterial populations that have the same species composition and relative abundance with those of the computational counterparts in panel A. Scale bar: 0.3 mm.

the former was attributed to the better growth and higher nisin resistance of the responder cRS compared to the responder iRS (Supplementary Figure S11); the latter was due to the fact that the cRS responder produces RFP constitutively while the iRS requires nisin induction for RFP expression. We further examined how the patterns of cellular lawns develop in the absent of nisin production by studying ecosystems composed of two responders, including the case of cGS and cRS (Row 3) and cGS and iRS (Row 4). Comparison of the resulting patterns with those in Row 1 and Row 2 suggests that the rich spatial structures of the consortia observed in Row 1 and Row 2 were mediated by the gene circuits through nisin production rather than the heterogeneity of cellular populations in space. To evaluate the reproducibility of the above results, we repeated all of the experiments, which resulted in spatial community structures (Supplementary Figure S22) that are consistent to those in Figure 4B. Collectively, the experimental results (Figure 4B and Supplementary Figure S22) confirmed the predictions of our simulations (Figure 4A and Supplementary Figure S20), demonstrating that the tunability and robustness of our synthetic circuits conferred the predictability for spatial organization of synthetic communities.

Harnessing the circuits to program controllable arrays of cellular stripes and spots

A fundamental goal of tissue and cellular engineering is to control the position, growth and subsequent function of living cells (30), which can be achieved through the creation of defined morphogen gradients in space. Given the robustness and tunability of our synthetic circuits, we set out to explore their utility in generating controllable spatial patterns of morphogens. Using a pair of nisin producer (PiG) and sensitive responder (iRS), we created cellular grids on agar plates by seeding the producer vertically and the responder horizontally (see Materials and Methods for details) (Figure 5A). Figure 5B–E shows the resulting fluorescence patterns upon 16 hours of incubation. Notably, as the spacing between the vertical green fluorescence stripes increases (the spacing for red remains constant), the horizontal red fluorescence patterns between neighboring green stripes vary accordingly from voids (panel B) to single continuous stripes (panel C) and to disconnected and repulsive twin stripes (panels D and E). The emergence of these distinct stripe arrays is attributed to the nisin responsive and sensitive characteristics of the responder (Supplementary Discussion). Using the same producer-responder pair, we also programmed cellular droplet arrays by surrounding the producer with the responder following a hexagonal pattern (see Materials and Methods for details) (Figure 5F). As shown in Figure 5G-K, by tuning the size and density of the producer droplets (green) (those of responder cells are fixed), we directed the responder cells (red) to form distinct patterns from voids (panel G), to triple arches (panel H), to full bright circles (panel I), to triangles surrounded with arcs (panel J), and to voids again (panel K). Using the same setup as Figure 5, we also employed another producer-responder pair, PiG and cRS, to program the spatial patterns of stripes (Supplementary Figure S23) and spots (Supplementary Figure S24). The alteration of these patterns is again due to the nisin responsive and sensitive features of the responder (Supplementary Discussion). In parallel to the experimental exploration, our mathematical model was able to successfully simulate both classes of controllable patterns (Supplementary Figures S25 and S26). Through the above experiments, we demonstrated that our synthetic circuits can be utilized for programming complex spatial biological patterns.

DISCUSSION

In this paper, we have presented synthetic gene circuits for spatial patterning that are simple in design and construction but are robust and tunable in functioning. The circuits required only minimal DNA parts for assembly, but produced desired patterns without the need for architectural fine tuning. In addition, they were robust against the perturbations

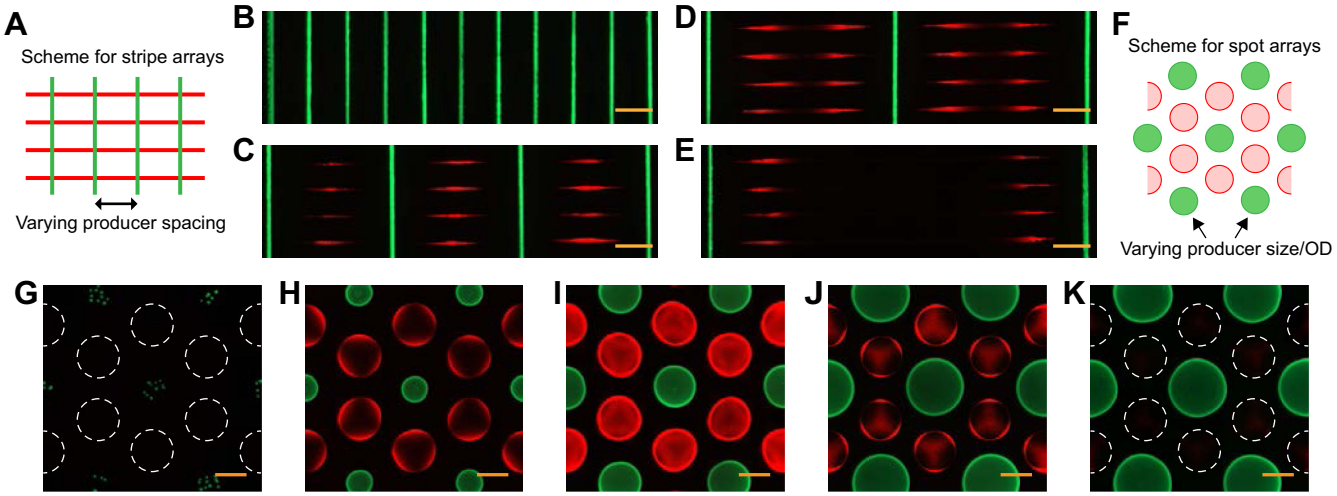

Figure 5. Controllable spatial arrays of stripes and spots programmed with the engineered producer (PiG) and responder (iRS) cells. (**A**). Schematic for the initial setup of stripe arrays. (**B–E**) Differential patterns of red fluorescence stripes (responder cells) develop with the increase of the spacing between the green fluorescence strips (producer cells). Scale bar: 4 mm. (**F**) Schematic for the initial setup of spot arrays. (**G–K**). Distinct patterns of red spots (responder cells) form with the alteration of the green spots (producer cells). Scale bar: 4 mm. Each experiment was repeated at least three times. Representative images from experiments are shown.

of various environmental factors (e.g. media composition, pH value, and temperature) and the variations of cellular contexts (e.g. the host organism and plasmid copy number). Moreover, although robust, the circuits were highly tunable to designed regulatory signals. Conferred by its robustness and tunability, the circuits further allowed us to establish predictable spatial structures of synthetic bacterial communities and to create controllable arrays of cellular grids and spots in space. Compared to other examples constructed to control spatial band behaviors (12,17–19), this study provides a simple and yet reliable solution to program robust and tunable spatial patterns that can be harnessed to create complex structures of populations. Circuit fragility is one of the major hurdles in synthetic biology, hampering the construction of complex networks for advanced functionalities and the applications of synthetic biology in real-world settings (10,31–34). To address the challenge, developing new design principles and methodologies have been the major efforts. This study demonstrates that deep mining of the untapped capacities of natural systems, such as the dual functionalities of nisin, can be an alternative strategy to build robustness. Importantly, with appropriate mining, implementation of desired functionality may not require complex circuit construction and optimization.

This work advances our capacity in controlling microbial communities and sensing environmental signals. It may also benefit the development of tissue engineering and biomaterial fabrications that require spatiotemporal control of signaling molecules. In addition, as the band-pass behavior of the engineered circuits is commonly occurring in nature, the study provides insights into the fundamental cellular coordination processes of natural systems, such as microbial community assembly and embryo development.

SUPPLEMENTARY DATA

Supplementary Data are available at NAR Online.

ACKNOWLEDGEMENTS

The authors thank Mr Gerald Axelbaum and Ms Ellen Schapiro for their generous financial support through the Brain and Behavior Research Foundation.

FUNDING

National Science Foundation [1227034, 1553649]; Office of Naval Research [N000141612525]; American Heart Association [12SDG12090025]; Brain and Behavior Research Foundation (NARSAD Young Investigator Award). Funding for open access charge: National Science Foundation.
Conflict of interest statement. None declared.

REFERENCES

1. Koch,A. and Meinhardt,H. (1994) Biological pattern formation: from basic mechanisms to complex structures. *Rev. Mod. Phys.*, **66**, 1481.
2. Ben-Jacob,E., Cohen,I. and Gutnick,D.L. (1998) Cooperative organization of bacterial colonies: from genotype to morphotype. *Annu. Rev. Microbiol.*, **52**, 779–806.
3. Campos-Ortega,J.A. and Hartenstein,V. (2013) *The Embryonic Development of Drosophila melanogaster*. Springer, Berlin.
4. Murray,J.D. (2001) *Mathematical Biology. II Spatial Models and Biomedical Applications*. Springer, Berlin.
5. Endy,D. (2005) Foundations for engineering biology. *Nature*, **438**, 449–453.
6. Arkin,A. (2008) Setting the standard in synthetic biology. *Nat. Biotechnol.*, **26**, 771–773.
7. Slusarczyk,A.L., Lin,A. and Weiss,R. (2012) Foundations for the design and implementation of synthetic genetic circuits. *Nat. Rev. Genet.*, **13**, 406–420.
8. Riccione,K.A., Smith,R.P., Lee,A.J. and You,L. (2012) A synthetic biology approach to understanding cellular information processing. *ACS Synth. Biol.*, **1**, 389–402.
9. Liu,C., Fu,X. and Huang,J.-D. (2013) Synthetic biology: a new approach to study biological pattern formation. *Quant Biol.*, **1**, 246–252.
10. Brophy,J.A. and Voigt,C.A. (2014) Principles of genetic circuit design. *Nat. Methods*, **11**, 508–520.

11. Kong,W., Celik,V., Liao,C., Hua,Q. and Lu,T. (2014) Programming the group behaviors of bacterial communities with synthetic cellular communication. *Bioresour. Bioprocess*, **1**, 1–11.
12. Basu,S., Gerchman,Y., Collins,C.H., Arnold,F.H. and Weiss,R. (2005) A synthetic multicellular system for programmed pattern formation. *Nature*, **434**, 1130–1134.
13. Danino,T., Mondragón-Palomino,O., Tsimring,L. and Hasty,J. (2010) A synchronized quorum of genetic clocks. *Nature*, **463**, 326–330.
14. Liu,C., Fu,X., Liu,L., Ren,X., Chau,C.K., Li,S., Xiang,L., Zeng,H., Chen,G. and Tang,L.-H. (2011) Sequential establishment of stripe patterns in an expanding cell population. *Science*, **334**, 238–241.
15. Cao,Y., Ryser,M.D., Payne,S., Li,B., Rao,C.V. and You,L. (2016) Collective space-sensing coordinates pattern scaling in engineered bacteria. *Cell*, **165**, 620–630.
16. Tabor,J.J., Salis,H.M., Simpson,Z.B., Chevalier,A.A., Levskaya,A., Marcotte,E.M., Voigt,C.A. and Ellington,A.D. (2009) A synthetic genetic edge detection program. *Cell*, **137**, 1272–1281.
17. Sohka,T., Heins,R.A., Phelan,R.M., Greisler,J.M., Townsend,C.A. and Ostermeier,M. (2009) An externally tunable bacterial band-pass filter. *Proc. Natl. Acad. Sci. U.S.A.*, **106**, 10135–10140.
18. Greber,D. and Fussenegger,M. (2010) An engineered mammalian band-pass network. *Nucleic Acids Res.*, gkq671.
19. Schaerli,Y., Munteanu,A., Gili,M., Cotterell,J., Sharpe,J. and Isalan,M. (2014) A unified design space of synthetic stripe-forming networks. *Nat. Commun.*, **5**, 4905.
20. Lubelski,J., Rink,R., Khusainov,R., Moll,G. and Kuipers,O. (2008) Biosynthesis, immunity, regulation, mode of action and engineering of the model lantibiotic nisin. *Cell Mol. Life Sci.*, **65**, 455–476.
21. Le Loir,Y., Gruss,A., Ehrlich,S. and Langella,P. (1998) A nine-residue synthetic propeptide enhances secretion efficiency of heterologous proteins in *Lactococcus lactis*. *J. Bacteriol.*, **180**, 1895–1903.
22. Stoddard,G.W., Petzel,J.P., Van Belkum,M., Kok,J. and McKay,L.L. (1992) Molecular analyses of the lactococcin A gene cluster from *Lactococcus lactis* subsp. *Lactis* biovar diacetylactis WM4. *Appl. Environ. Microbiol.*, **58**, 1952–1961.
23. Kong,W., Kapuganti,V.S. and Lu,T. (2015) A gene network engineering platform for lactic acid bacteria. *Nucleic Acids Res.*, **44**, e37.
24. van de Guchte,M., Van der Vossen,J., Kok,J. and Venema,G. (1989) Construction of a lactococcal expression vector: expression of hen egg white lysozyme in *Lactococcus lactis* subsp. *lactis*. *Appl. Environ. Microbiol.*, **55**, 224–228.
25. Kong,W. and Lu,T. (2014) Cloning and optimization of a nisin biosynthesis pathway for bacteriocin harvest. *ACS Synth. Biol.*, **3**, 439–445.
26. Kitano,H. (2004) Biological robustness. *Nat. Rev. Genet.*, **5**, 826–837.
27. Brenner,K., You,L. and Arnold,F.H. (2008) Engineering microbial consortia: a new frontier in synthetic biology. *Trends Biotechnol.*, **26**, 483–489.
28. Balagaddé,F.K., Song,H., Ozaki,J., Collins,C.H., Barnet,M., Arnold,F.H., Quake,S.R. and You,L. (2008) A synthetic *Escherichia coli* predator–prey ecosystem. *Mol. Syst. Biol.*, **4**, 187.
29. Chen,Y., Kim,J.K., Hirning,A.J., Josić,K. and Bennett,M.R. (2015) Emergent genetic oscillations in a synthetic microbial consortium. *Science*, **349**, 986–989.
30. Langer,R. and Vacanti,J.P. (1993) Tissue engineering. *Science*, **260**, 920–926.
31. Serrano,L. (2007) Synthetic biology: promises and challenges. *Mol. Syst. Biol.*, **3**, 158.
32. Lu,T.K., Khalil,A.S. and Collins,J.J. (2009) Next-generation synthetic gene networks. *Nat. Biotechnol.*, **27**, 1139–1150.
33. Kwok,R. (2010) Five hard truths for synthetic biology. *Nature*, **463**, 288.
34. Ruder,W.C., Lu,T. and Collins,J.J. (2011) Synthetic biology moving into the clinic. *Science*, **333**, 1248–1252.